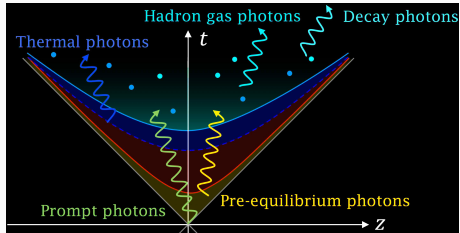


Magnetic fields in heavy-ion collisions: catalyzers of photon production via gluon fusion

Malena Tejeda-Yeomans

Facultad de Ciencias
Universidad de Colima
México



Context

Prompt photon yield and elliptic flow from gluon fusion induced by magnetic fields in relativistic heavy-ion collisions.

A. Ayala, J. Castaño, C. Domínguez, L. Hernández, S. Hernández, METY.

PRD 96 (2017) 1, PRD 96 (2017) 11; e-Print: 1704.02433 [hep-ph]

2020



Centrality dependence of photon yield and elliptic flow from gluon fusion and splitting induced by magnetic fields in relativistic heavy-ion collisions.

A. Ayala, J. Castaño, I. Domínguez, J. Salinas, METY. EPJA 56 (2020); e-Print: 1904.02938 [hep-ph]

2015



Anisotropic photon emission from gluon fusion and splitting in a strong magnetic background: The two-gluon one-photon vertex.

A. Ayala, J. Castaño, L. Hernández, A. Mizher, METY, R. Zamora.

PRC 106 (2022); e-Print: 2209.09364 [hep-ph]

2010

2005

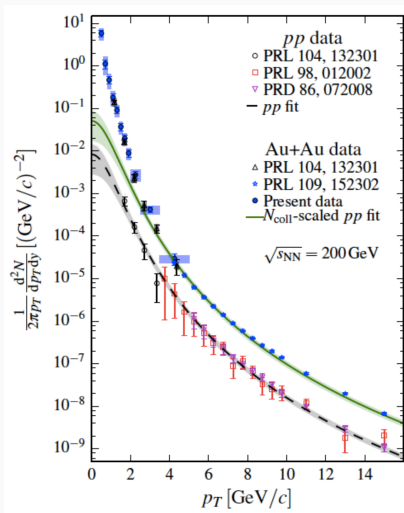
2000

1995

Earlier



Connections: PHENIX@BNL - PRC 91 (2015)



2020



2015



2010

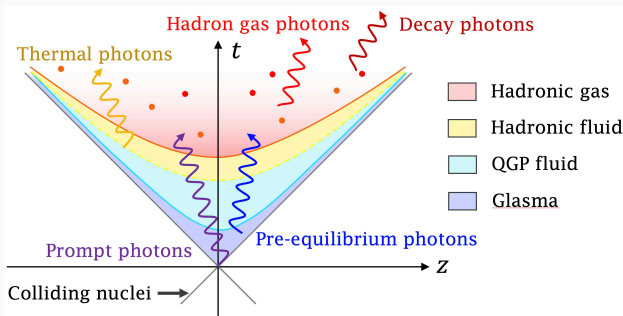
2005

2000

1995

Earlier

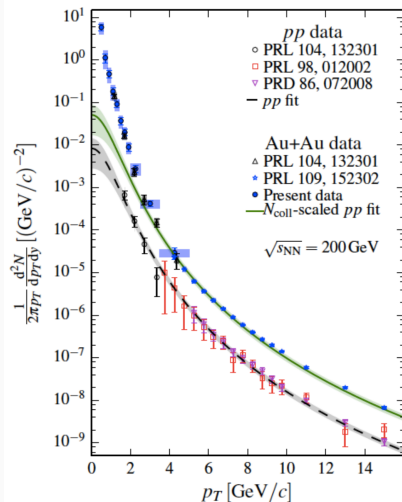




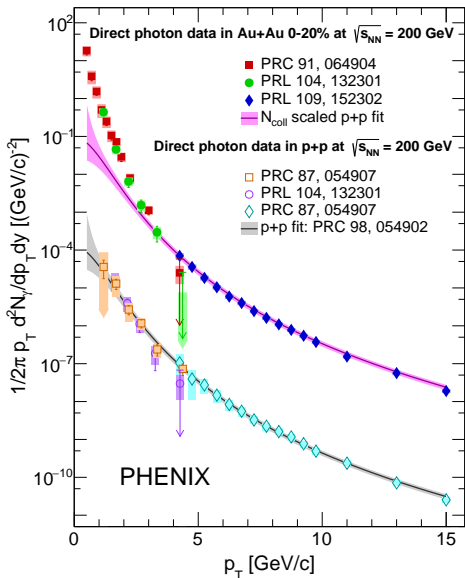
- decay photons: approx 80-90% of all the photons produced in HICs
- direct photons:
 - prompt photons: sources similar to those in $p + p$, scale as N_{coll}
 - non-prompt: thermal from HG and QGP, jet-medium intns and from pre-equilibrium

HIC system evolution: expands and cools, earlier phases - higher temperatures and likely dominated by emissions at higher p_T . A. Monnai, Int.J.Mod.Phys.A37 (2022)

PHENIX@BNL γ -yield



PRC 91 (2015)

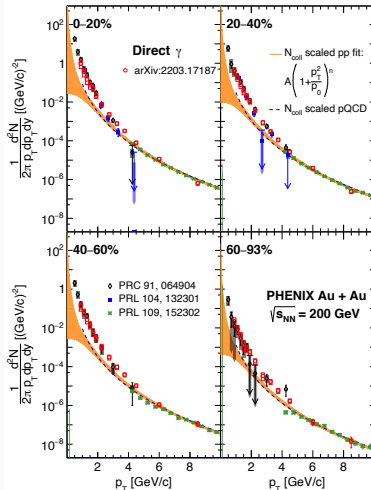
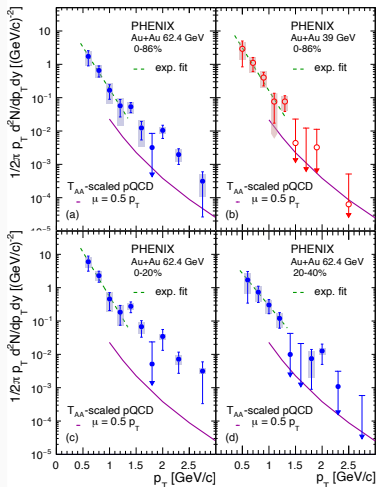


PRC 107 (2023)

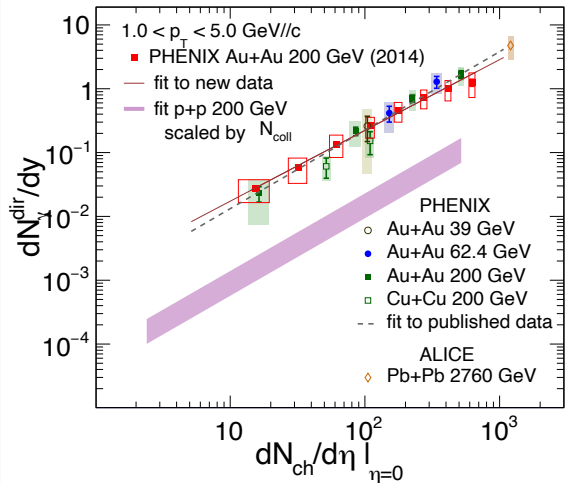
ALL

PHENIX@BNL direct γ -yield (2022)

Au+Au at $\sqrt{s_{NN}} = 39$ GeV and $\sqrt{s_{NN}} = 64$ GeV (2203.12354 [nucl-ex]) and for $\sqrt{s_{NN}} = 200$ GeV (2203.17187 [nucl-ex]) for different collision centralities.



Universal scaling behavior of direct γ -yield in all A+A systems



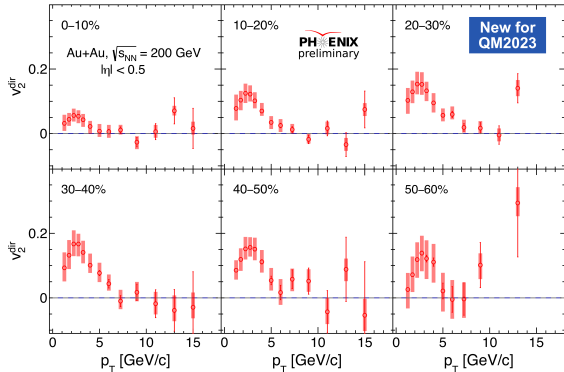
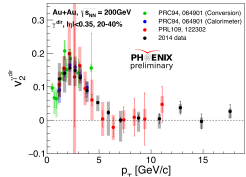
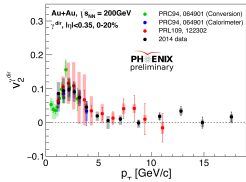
$$\frac{dN_\gamma}{dy} = A \left(\frac{dN_{ch}}{d\eta} \right)^\alpha$$

$$\alpha = 1.11 \pm 0.02(stat)_{-0.08}^{+0.09}(sys)$$

arxiv 2203.17187

Vassu Doomra (Stonybrook U), QM23. [Check out their talk here](#)

Direct Photons v_2



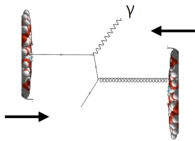
Direct photons v_2 in the high p_T region is consistent with zero within uncertainties.

“Direct photon puzzle”: exp status (2023)

- Direct photons have large yield and azimuthal anisotropy at low p_T
- after subtracting the prompt photon component, the inverse slope for the p_T range from 1-2 GeV/ c is 250 MeV/ c , but increases to about 400 MeV/ c for the range from 2 to 4 GeV/ c .
- within the experimental uncertainty, there is no indication of a system size dependence of the inverse slope.
- the system size dependence of the yield, expressed through the power α , remains independent of p_T over the entire observed range from 1 to 6 GeV/ c .

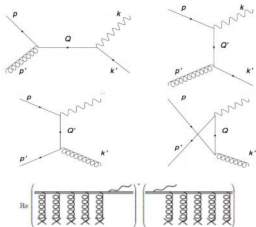
These features are qualitatively consistent with the emission of thermal photons from the QGP, but elude a quantitative description through theoretical model calculations.

Direct photons: prompt + thermal + non-cocktail



Prompt Photons

LO: AMY JHEP **0112**, 009, (2001).



NLO: J. Ghiglieri et al., JHEP **1305**, 010 (2013).

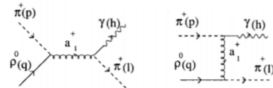


Thermal Photons: Produced in

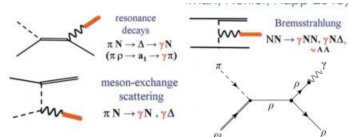
QGP stage.

ECT - Strongly intrn matter in extreme B-fields (2023)

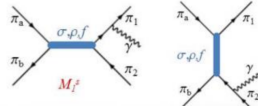
TRG, Phys. Rev. C **69**, 014903 (2004).



R. Rapp and J. Wambach, Eur. Phys. J. A **6**, 415 (1999).



W. Liu and R. Rapp, Nucl. Phys. A **796**, 101 (2007).

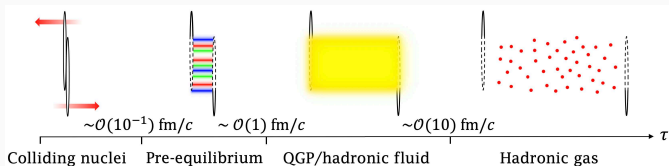


Non-Cocktail: Early hadronic decay.

5

images from Jorge Castaño

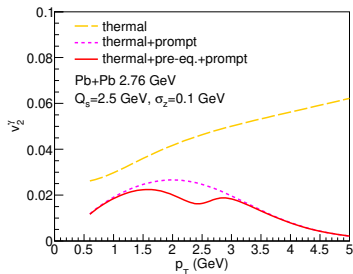
Pre-equilibrium photons



In the pre-equilibrium stage: large number of gluons (glasma) and fewer quarks (parametric proportionality in α_s).

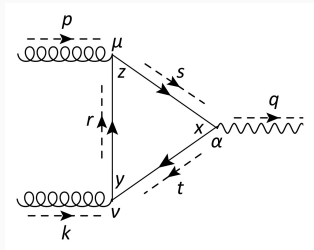
$2 \rightarrow 2$ scattering processes involving quarks and gluons in this stage can give rise to an excess (over conventional sources) of photons.

The photon yield increases, but v_2 worsens.



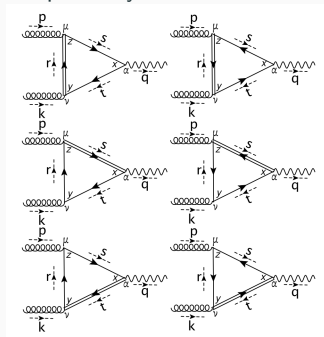
Akihiko Monnai, Int. J. Mod. Phys. A 37 (2022)

New photoproduction channel opens in pre-equilibrium stage

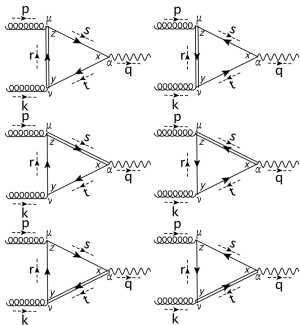


coupling between two gluons and one photon is possible by the presence of the external magnetic field (in the $B \rightarrow 0$ limit we recover Furry's theorem, QED and QCD have charge conjugation symmetry)

Idea: magnetic field induced processes + large abundance of soft pre-equilibrium gluons \rightarrow enhance the photon yield and ν_2



Gluon fusion + strong magnetic field - calculation set up



$$iS(p) = \int_0^\infty \frac{d\tau}{\cos(|eq_f B| \tau)} e^{i\tau \left[p_{\parallel}^2 - p_{\perp}^2 \frac{\tan(|eq_f B| \tau)}{|eq_f B| \tau} - m_f^2 + i\epsilon \right]} \times \left\{ \begin{aligned} & [\cos(|eq_f B| \tau) + \gamma_1 \gamma_2 \sin(|eq_f B| \tau)] (m_f + \not{p}_{\parallel}) \\ & - \frac{\not{p}_{\perp}}{\cos(|eq_f B| \tau)} \end{aligned} \right\} \quad \text{where} \quad (1)$$

$$\Phi(x, x') = \text{Exp} \left\{ ieq_f \int_{x'}^x d\xi^\mu \left[A_\mu + \frac{1}{2} F_{\mu\nu} (\xi - x')^\nu \right] \right\} \quad (2)$$

magnetized propagator \rightsquigarrow Furry's theorem no longer applies, non-vanishing process probability

$$\begin{aligned} \widetilde{M}_{gg \rightarrow \gamma} = & - \int d^4x d^4y d^4z \int \frac{d^4r}{(2\pi)^4} \frac{d^4s}{(2\pi)^4} \frac{d^4t}{(2\pi)^4} e^{-it \cdot (y-x)} e^{-is \cdot (x-z)} e^{-ir \cdot (z-y)} e^{-ip \cdot z} e^{-ik \cdot y} e^{iq \cdot x} \\ & \left\{ \text{Tr} \left[ieq_f \gamma_\alpha iS_{ac}(s) ig \gamma_\mu t^c iS_{cd}(r) ig \gamma_\nu t^d iS_{da}(t) \right] + \text{Tr} \left[ieq_f \gamma_\alpha iS_{ad}(t) ig \gamma_\nu t^d iS_{dc}(r) ig \gamma_\mu t^c iS_{ca}(s) \right] \right\} \\ & \times \Phi(x, y) \Phi(y, z) \Phi(z, x) \epsilon^\mu(\lambda_p) \epsilon^\nu(\lambda_k) \epsilon^\alpha(\lambda_q) \end{aligned} \quad (3)$$

Gluon fusion + strong magnetic field - calculation set up

- initially, take a constant magnetic field in the z-direction
- at the earliest times, when thermalization has not been achieved, the magnetic field is the dominant internal energy scale in the process
- calculation accounts for photons coming from the *glasma*, where gluons are described by a dense, non-equilibrium state

in the massless limit ($m_f \rightarrow 0$)

$$iS_{ab}^{(0)}(p) = i \frac{e^{-p_{\perp}^2 / eq_f B}}{p_{\parallel}^2} \delta_{ab} \not{p}_{\parallel} \mathcal{O}^-, \quad \mathcal{O}^{(\pm)} = \left[1 \pm i\gamma^1 \gamma^2 \text{sign}(eq_f B) \right] / 2 \quad (4)$$

$$iS_{ab}^{(1)}(p) = -2i \frac{e^{-p_{\perp}^2 / eq_f B}}{p_{\parallel}^2 - 2|eq_f B|} \delta_{ab} \left[\not{p}_{\parallel} \mathcal{O}^- \left(1 - \frac{2p_{\perp}^2}{|eq_f B|} \right) - \not{p}_{\parallel} \mathcal{O}^+ + 2\not{p}_{\perp} \right] \quad (5)$$

- in the absence of thermal effects, and with $|eq_f B| \gg m_f^2$, work using the quark propagators in the lowest Landau level (LLL)
- first non-vanishing term: one of the quarks in the loop is in the first excited Landau level (1LL)

The matrix element is

$$\begin{aligned}
 \widetilde{\mathcal{M}}_{gg \rightarrow \gamma} &= 8i(2\pi)^4 \delta^{(4)}(q - k - p) \delta^{cd} e q_f g^2 \\
 &\times \int \frac{d^4 r}{(2\pi)^4} \frac{d^4 s}{(2\pi)^4} \frac{d^4 t}{(2\pi)^4} \epsilon^\mu(\lambda_p) \epsilon^\nu(\lambda_k) \epsilon^\alpha(\lambda_q) \\
 &\times \int d^4 w d^4 l e^{-il(r-t-k)} e^{-iw(r-s+p)} \\
 &\times \exp \left\{ -i \frac{|eq_f B|}{2} \epsilon_{mj} w_m l_j \right\} \exp \left\{ -\frac{r_\perp^2 + s_\perp^2 + t_\perp^2}{|eq_f B|} \right\} \\
 &\times \text{Tr} \left\{ \frac{\gamma_1 \gamma_2 \gamma_\alpha \not{t}_\perp \gamma_\nu \not{t}_\parallel \gamma_\mu \not{s}_\parallel}{r_\parallel^2 s_\parallel^2 (t_\parallel^2 - 2|eq_f B|)} + \frac{\gamma_1 \gamma_2 \gamma_\mu \not{s}_\perp \gamma_\alpha \not{t}_\parallel \gamma_\nu \not{t}_\parallel}{t_\parallel^2 r_\parallel^2 (s_\parallel^2 - 2|eq_f B|)} \right. \\
 &\left. + \frac{\gamma_1 \gamma_2 \gamma_\nu \not{t}_\perp \gamma_\mu \not{s}_\parallel \gamma_\alpha \not{t}_\parallel}{s_\parallel^2 t_\parallel^2 (r_\parallel^2 - 2|eq_f B|)} \right\} \epsilon_\mu(\lambda_p) \epsilon_\nu(\lambda_k) \epsilon_\alpha(\lambda_q) \quad (6)
 \end{aligned}$$

For low p_T external photons: $2|eq_f B| \gg t_{\parallel}^2, s_{\parallel}^2, r_{\parallel}^2$

A. Ayala, J. Castano-Yepes, I. Dominguez, J. Salinas, METY. EPJ A 56 (2020); 1904.02938 [hep-ph]

$$\begin{aligned}
 \widetilde{\mathcal{M}}_{gg \rightarrow \gamma} &= -i(2\pi)^4 \delta^{(4)}(q - k - p) \frac{eq_f g^2 \delta^{cd} e^{f(p_{\perp}, k_{\perp})}}{32\pi(2\pi)^8} \\
 \times & \left\{ \left(g_{\parallel}^{\mu\alpha} - \frac{p_{\parallel}^{\mu} p_{\parallel}^{\alpha}}{p_{\parallel}^2} \right) h^{\nu}(a) - \left(g_{\parallel}^{\mu\nu} - \frac{p_{\parallel}^{\mu} p_{\parallel}^{\nu}}{p_{\parallel}^2} \right) h^{\alpha}(a) \right. \\
 + & \left(g_{\parallel}^{\mu\nu} - \frac{k_{\parallel}^{\mu} k_{\parallel}^{\nu}}{k_{\parallel}^2} \right) h^{\alpha}(b) - \left(g_{\parallel}^{\alpha\nu} - \frac{k_{\parallel}^{\alpha} k_{\parallel}^{\nu}}{k_{\parallel}^2} \right) h^{\mu}(b) \\
 + & \left. \left(g_{\parallel}^{\alpha\nu} - \frac{q_{\parallel}^{\alpha} q_{\parallel}^{\nu}}{q_{\parallel}^2} \right) h^{\mu}(c) - \left(g_{\parallel}^{\mu\alpha} - \frac{q_{\parallel}^{\mu} q_{\parallel}^{\alpha}}{q_{\parallel}^2} \right) h^{\nu}(c) \right\} \\
 \times & \epsilon_{\mu}(\lambda_p) \epsilon_{\nu}(\lambda_k) \epsilon_{\alpha}(\lambda_q)
 \end{aligned} \tag{7}$$

Gluon fusion/splitting + strong B field - calculation set up

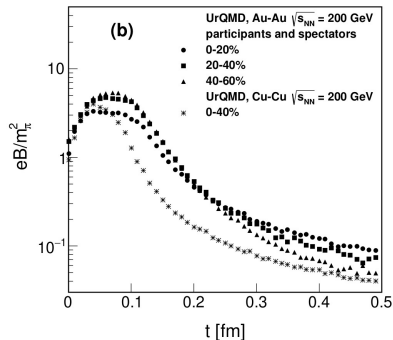
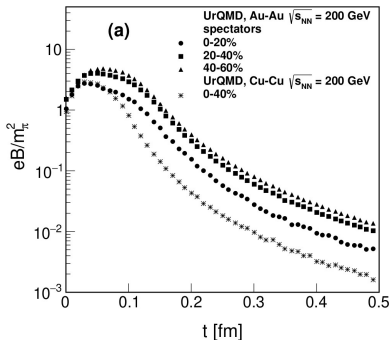
The invariant photon momentum distribution is given by

$$\omega_q \frac{dN^{\text{mag}}}{d^3q} = \frac{\mathcal{V}\Delta\mathcal{T}}{2(2\pi)^3} \int \frac{d^3p}{(2\pi)^3 2\omega_p} \int \frac{d^3k}{(2\pi)^3 2\omega_k} (2\pi)^4 \left\{ \delta^{(4)}(q - k - p) n(\omega_p) n(\omega_k) \sum_{c,p,f} \overline{|\mathcal{M}_{gg \rightarrow \gamma}|^2} + \delta^{(4)}(q + k - p) n(\omega_p) [1 + n(\omega_k)] \sum_{c,p,f} \overline{|\mathcal{M}_{g \rightarrow g\gamma}|^2} \right\} \quad (8)$$

- $\mathcal{V}\Delta\mathcal{T}$: space-time volume where the reaction takes place, spatial volume of the nuclear overlap region $\mathcal{V}(t)$ at time t and the time interval
- $\Delta\mathcal{T}$ where the magnetic field, taken as having a constant intensity $B(t)$.
- overall lifetime $\Delta\mathcal{T}$ can be estimated calculating the duration of the magnetic pulse

detail

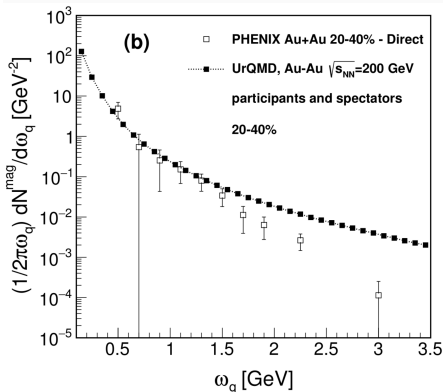
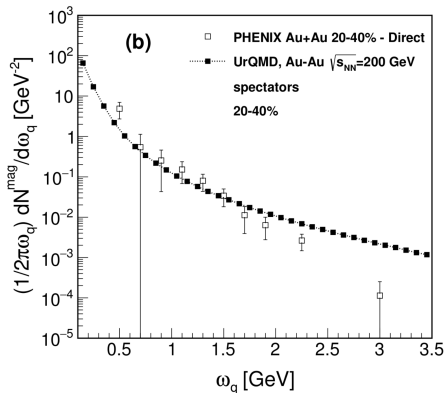
Field strength as a function of time: Lienard-Wiechert potential UrQMD



A. A., J.D. Castaño, I. Dominguez, L.A. Hernández, J. Salinas, M.E. Tejada-Yeomans, Eur. Phys. J. A 56, 53 (2020).

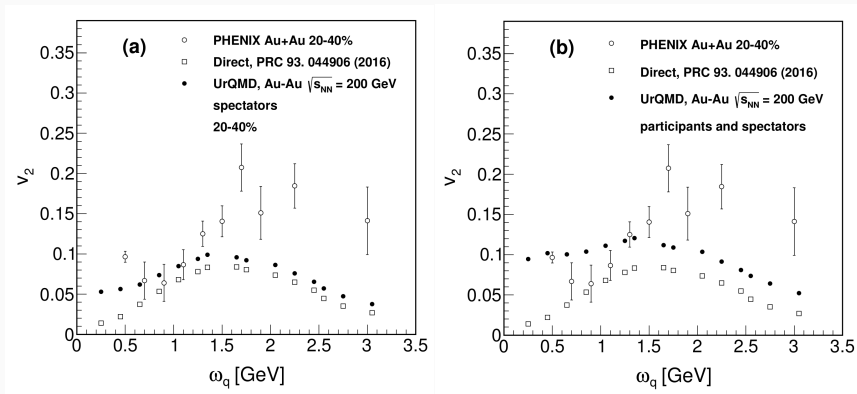
Gluon fusion/splitting + strong magnetic field - yield

A. Ayala, J. Castano-Yepes, I. Dominguez, J. Salinas, METY. EPJ A 56 (2020); 1904.02938 [hep-ph]



Gluon fusion/splitting + strong magnetic field - v_2

A. Ayala, J. Castano-Yepes, I. Dominguez, J. Salinas, METY. EPJ A 56 (2020); 1904.02938 [hep-ph]



v_2 as a weighted average accounting for magnetic + direct photons

[Back](#)

$$v_2(\omega_q) = \frac{\sum_{i=1}^m \left[\frac{dN}{d\omega_q} \right]_i [v_2^{\text{mag}}(\omega_q)]_i + \frac{dN^{\text{direct}}}{d\omega_q}(\omega_q) v_2^{\text{direct}}(\omega_q)}{\sum_{i=1}^m \left[\frac{dN}{d\omega_q} \right]_i + \frac{dN^{\text{direct}}}{d\omega_q}(\omega_q)}$$

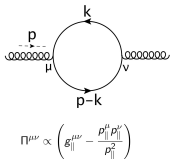
1L 2g1 γ vertex + strong magnetic field - improvement!

For low p_T external photons: $2|eq_f B| \gg t_{\parallel}^2, s_{\parallel}^2, r_{\parallel}^2$

A. Ayala, J. Castano-Yepes, L.A. Hernandez, A. Mizher, METY, R. Zamora. PRC 106 (2022); e-Print: 2209.09364 [hep-ph]

In strong \vec{B} case: 2 external particles with longitudinal and a third one with transverse polarizations

Starting from the two-gluon polarization tensor $\Pi^{\mu\nu}$ in the strong field limit



Lots of nice work done!

K. Hattori, et al. Symmetry 14 (2022); PRD 97, 014023 (2018)

I. Shovkovy, et al. Particles 5 (2022); PRD 106 (2022)

$$\Gamma_{ab}^{\mu\nu\alpha} = \delta_{ab} \Gamma^{\mu\nu\alpha},$$

$$\begin{aligned} \Gamma^{\mu\nu\alpha} &\equiv \Gamma_1(\omega_q, \omega_k, q^2) \frac{\epsilon_{ij} q_{\perp}^i g_{\perp}^{j\mu}}{\sqrt{q_{\perp}^2}} \left(g_{\parallel}^{\nu\alpha} - \frac{q_{\parallel}^{\nu} q_{\parallel}^{\alpha}}{q_{\parallel}^2} \right) \\ &+ \Gamma_2(\omega_q, \omega_k, q^2) \frac{\epsilon_{ij} q_{\perp}^i g_{\perp}^{j\nu}}{\sqrt{q_{\perp}^2}} \left(g_{\parallel}^{\mu\alpha} - \frac{q_{\parallel}^{\mu} q_{\parallel}^{\alpha}}{q_{\parallel}^2} \right) \\ &+ \Gamma_3(\omega_q, \omega_k, q^2) \frac{\epsilon_{ij} q_{\perp}^i g_{\perp}^{j\alpha}}{\sqrt{q_{\perp}^2}} \left(g_{\parallel}^{\mu\nu} - \frac{q_{\parallel}^{\mu} q_{\parallel}^{\nu}}{q_{\parallel}^2} \right) \end{aligned}$$

$$\Gamma_n \equiv \frac{8\pi^4 q_f g^2}{|eq_f B|} e^{f(p_{\perp}, k_{\perp})} |q_{\perp}| \tilde{\Gamma}_n(\omega_q, \omega_k, \theta)$$

1L 2g1 γ vertex + strong magnetic field - improvement!

In the strong field approximation, the physical picture that emerges is:

- a strong magnetic field forces two of the vector particles to occupy parallel polarization states (K. Hattori and D. Satow, PRD 97 (2018); K. Fukushima, PRD 83 (2011))
- when the vertex involves a third vector particle, invariance under charge conjugation and conservation of angular momentum require that its polarization state is transverse
- one of the quarks that make up the loop needs to be placed not in the LLL but instead in the 1LL (if polarization is in the same direction: 3 spin 1/2 quarks in the loop cannot account for spin state of 3 vector particles) \rightarrow transverse mode of one vector particle

In the weak field limit, similar selection rules (S. L. Adler et al PRL 25, (1970))

1L 2g1 γ vertex + strong magnetic field - improvement!

The contributing Feynman diagrams, obtained when placing two fermion propagators in the LLL and the other in the 1LL, after integration of the configuration space variables, the vertex is given by

$$\Gamma_{ab}^{\mu\nu\alpha} = -\delta^{(4)}(q - k - p) \text{Tr}[t_a t_b] \frac{8\pi^4 q_f g^2}{|eq_f B|} q_{\parallel}^2 e^{f(p_{\perp}, k_{\perp})} \sum_{i=1}^3 D_i^{\mu\nu\alpha}, \quad (9)$$

We calculate $\Gamma_n(\omega_q, \omega_k, q^2)$ for $n = 1, 2, 3$ by projecting onto the basis

$$\left\{ v_{\perp}^{\mu} \Pi_{\parallel}^{\nu\alpha}, v_{\perp}^{\nu} \Pi_{\parallel}^{\mu\alpha}, v_{\perp}^{\alpha} \Pi_{\parallel}^{\mu\nu} \right\}, \quad (10)$$

$$\begin{aligned} v_{\perp}^{\mu} \Pi_{\parallel}^{\nu\alpha} D_{\mu\nu\alpha}^1 &= \frac{8\pi^4 q_f g^2}{|eq_f B|} q_{\parallel}^2 e^{f(p_{\perp}, k_{\perp})} |q_{\perp}| \tilde{C} \mathcal{I}_1, \\ v_{\perp}^{\nu} \Pi_{\parallel}^{\mu\alpha} D_{\mu\nu\alpha}^1 &= -\frac{8\pi^4 q_f g^2}{|eq_f B|} q_{\parallel}^2 e^{f(p_{\perp}, k_{\perp})} |q_{\perp}| \tilde{C} \mathcal{I}_1, \\ v_{\perp}^{\alpha} \Pi_{\parallel}^{\mu\nu} D_{\mu\nu\alpha}^1 &= 0, \end{aligned} \quad (11)$$

1L 2g1 γ vertex + strong magnetic field - improvement!

$$\begin{aligned}v_{\perp}^{\mu} \Pi_{\parallel}^{\nu\alpha} D_{\mu\nu\alpha}^2 &= -\frac{8\pi^4 q_f g^2}{|eq_f B|} q_{\parallel}^2 e^{f(p_{\perp}, k_{\perp})} |q_{\perp}| \tilde{B} \mathcal{I}_2, \\v_{\perp}^{\nu} \Pi_{\parallel}^{\mu\alpha} D_{\mu\nu\alpha}^2 &= 0, \\v_{\perp}^{\alpha} \Pi_{\parallel}^{\mu\nu} D_{\mu\nu\alpha}^2 &= \frac{8\pi^4 q_f g^2}{|eq_f B|} q_{\parallel}^2 e^{f(p_{\perp}, k_{\perp})} |q_{\perp}| \tilde{B} \mathcal{I}_2, \end{aligned} \quad (12)$$

$$\begin{aligned}v_{\perp}^{\mu} \Pi_{\parallel}^{\nu\alpha} D_{\mu\nu\alpha}^3 &= 0, \\v_{\perp}^{\nu} \Pi_{\parallel}^{\mu\alpha} D_{\mu\nu\alpha}^3 &= \frac{8\pi^4 q_f g^2}{|eq_f B|} q_{\parallel}^2 e^{f(p_{\perp}, k_{\perp})} |q_{\perp}| \tilde{A}_2 \mathcal{I}_3, \\v_{\perp}^{\alpha} \Pi_{\parallel}^{\mu\nu} D_{\mu\nu\alpha}^3 &= -\frac{8\pi^4 q_f g^2}{|eq_f B|} q_{\parallel}^2 e^{f(p_{\perp}, k_{\perp})} |q_{\perp}| \tilde{A}_2 \mathcal{I}_3. \end{aligned} \quad (13)$$

1L 2g1 γ vertex + strong magnetic field - improvement!

Using these results, we can go back to the vertex and collect the contributions that correspond to each coefficient $\Gamma_n(\omega_q, \omega_k, q^2)$. The projection with $v_{\perp}^{\mu} \Pi_{\parallel}^{\nu\alpha}$ from the three sets in (11)-(13), contributes to

$$\Gamma_1 \equiv \frac{8\pi^4 q_f g^2}{|eq_f B|} e^{f(p_{\perp}, k_{\perp})} |q_{\perp}| \tilde{\Gamma}_1(\omega_p, \omega_q, \theta). \quad (14)$$

The projection with $v_{\perp}^{\nu} \Pi_{\parallel}^{\mu\alpha}$ contributes to

$$\Gamma_2 \equiv \frac{8\pi^4 q_f g^2}{|eq_f B|} e^{f(p_{\perp}, k_{\perp})} |q_{\perp}| \tilde{\Gamma}_2(\omega_p, \omega_q, \theta), \quad (15)$$

the projection with $v_{\perp}^{\alpha} \Pi_{\parallel}^{\mu\nu}$, that contributes to

$$\Gamma_3 \equiv \frac{8\pi^4 q_f g^2}{|eq_f B|} e^{f(p_{\perp}, k_{\perp})} |q_{\perp}| \tilde{\Gamma}_3(\omega_p, \omega_q, \theta). \quad (16)$$

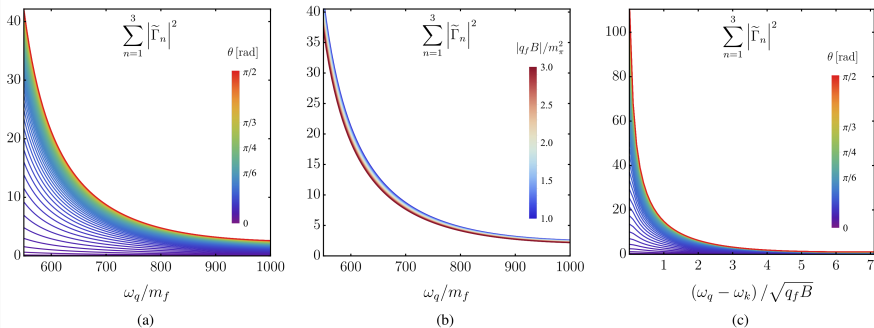
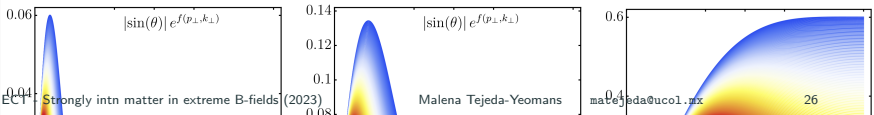


FIG. 3: Sum of squared amplitudes of $\tilde{\Gamma}_n$, $n = 1, 2, 3$ from Eqs. (B5), (B6) and (B7), as a function of: (a) the photon energy ω_q and the angle with respect to the magnetic field θ with $|q_f B| = m_\pi^2$, (b) the photon energy ω_q and the magnetic field strength $|q_f B|$ with $\theta = \pi/2$, and (c) the ratio $(\omega_q - \omega_k)/\sqrt{|q_f B|}$ and the angle with respect to the magnetic field θ with $|q_f B| = m_\pi^2$. All the physical parameters are normalized with the quarks mass $m_f = 2 \times 10^{-3}$ GeV, having fixed $\omega_k = 1$ GeV.



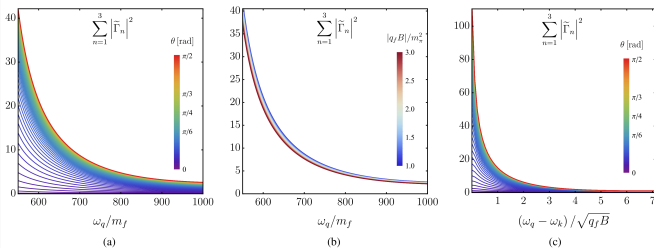


FIG. 3: Sum of squared amplitudes of $\tilde{\Gamma}_n$, $n = 1, 2, 3$ from Eqs. (B5), (B6) and (B7), as a function of: (a) the photon energy ω_q and the angle with respect to the magnetic field θ with $|q_f B| = m_\pi^2$, (b) the photon energy ω_q and the magnetic field strength $|q_f B|$ with $\theta = \pi/2$, and (c) the ratio $(\omega_q - \omega_k)/\sqrt{|q_f B|}$ and the angle with respect to the magnetic field θ with $|q_f B| = m_\pi^2$. All the physical parameters are normalized with the quarks mass $m_f = 2 \times 10^{-3}$ GeV, having fixed $\omega_k = 1$ GeV.

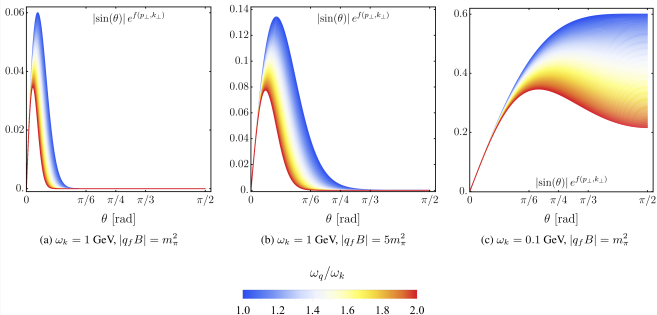


FIG. 4: Angular dependence of the factor $|q_\perp| e^{f(p_\perp, k_\perp)}$ of Eq. (38) as a function of the photon's energy ω_q and the angle with respect to the magnetic field θ for fixed values of ω_k and $|q_f B|$.

1L 2g1 γ vertex + strong magnetic field - improvement!

- $\sum |\tilde{\Gamma}_n|^2$ is larger for a photon propagation within the reaction plane ($\theta = \pi/2$) and that for $\theta = \pi/2$ it is also larger for smaller field intensities
- $|q_\perp|e^{f(\rho_\perp, k_\perp)}$ also depends on θ and peaks at small angles for large gluon energies, but here the square amplitude is highly suppressed close to the reaction plane
- for small gluon energies and/or a large field strength, the pre-factor is dominated by emission angles close to the reaction plane
- the pre-factor vanishes for $\theta = 0$, which prevents photons from being emitted along the direction of the magnetic field.
- Since at pre-equilibrium the largest gluon abundance happens for small energies, a positive v_2 coefficient may be expected

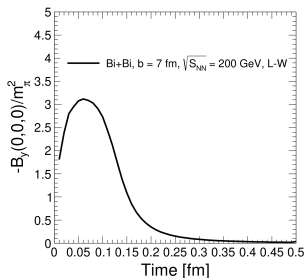
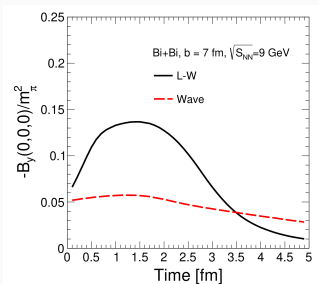
Estimation and simulation of B-fields in HIC

$\vec{B}(r_i, t)$ can be calculated using the Liénard-Wiechert potential generated by *non-accelerated* charges moving along the beam direction as

$$e\vec{B}(r_i, t) = \alpha_{em} \sum_j \frac{(1 - v_j^2) \vec{v}_j \times \vec{R}_j}{R_j^3 \left[1 - \frac{(\vec{v}_j \times \vec{R}_j)^2}{R_j^2} \right]^{3/2}},$$

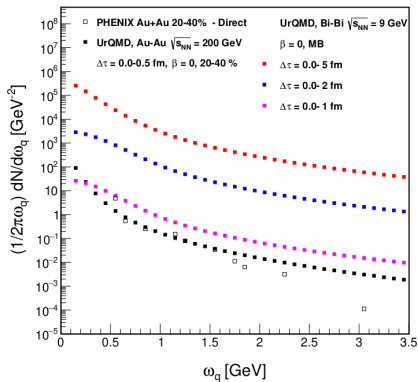
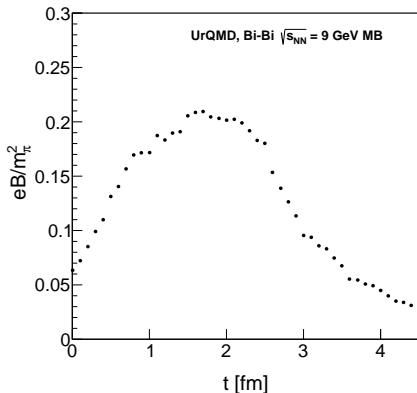
where $\vec{R}_j = \vec{r} - \vec{r}_j(t)$, $\vec{r}_j(t)$ is the position of the j -th charge moving with velocity \vec{v}_j and the sum runs over charged particles in each event.

Work in progress with A. Guirado, P. Nieto and I. Dominguez.



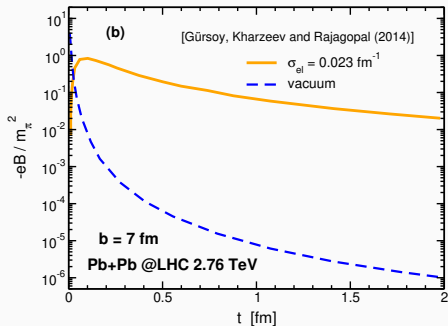
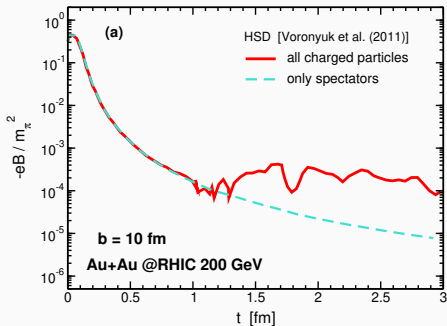
Gluon fusion/splitting + strong magnetic field - preliminary

Isabel Dominguez, Pedro Nieto - preliminary (Sep. 2023)



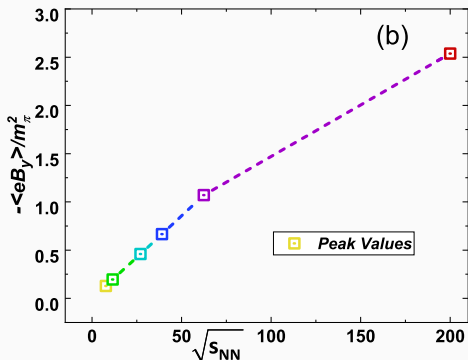
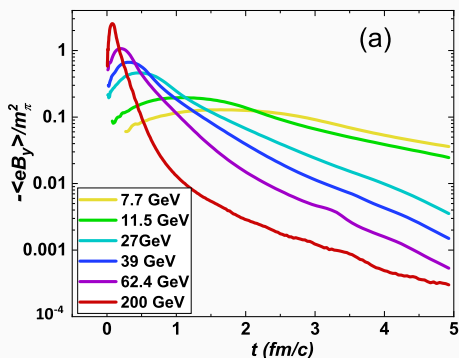
Magnetic fields in HIC

Lucia Oliva (Frankfurt U., Catania U.), *Electromagnetic fields and directed flow in large and small colliding systems at ultrarelativistic energies*, Eur.Phys.J.A 56 (2020), e-Print: 2007.00560 [nucl-th]



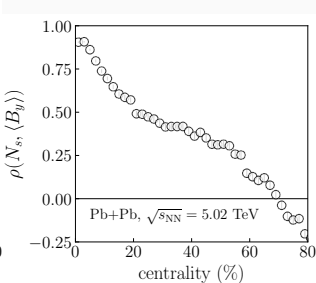
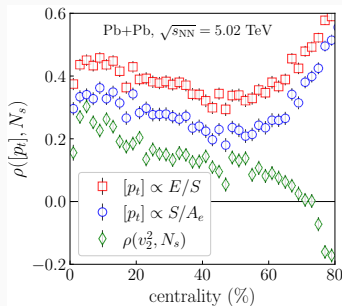
Magnetic fields in HIC

I. Siddique, X. Sheng, Q. Wang, *Space-average electromagnetic fields and electromagnetic anomaly weighted by energy density in heavy-ion collisions*, Phys.Rev.C 104 (2021), e-Print: 2106.00478 [nucl-th]



Magnetic fields in HIC

G. Giacalone, C. Shen, *Manipulating strong electromagnetic fields with the average transverse momentum of relativistic nuclear collisions*, Eur.Phys.J.A 57 (2021), e-Print: 2104.01890 [nucl-th]



$$\langle \vec{B} \rangle = \frac{1}{E} \int d^2x \vec{B}(x) e(x)$$

$$[p_t] = \frac{1}{N} \int d^2p_t \frac{dN}{d^2p_t} |p_t|$$

$\langle \rangle$ avg over events

Pearson coeff: stat correlation, energy density profiles with T_{RENT}o

$$\rho(o_1, o_2) = \frac{\langle \delta o_1 \delta o_2 \rangle}{\sqrt{\langle (\delta o_1)^2 \rangle} \sqrt{\langle (\delta o_2)^2 \rangle}} \quad \text{where} \quad \delta o = o - \langle o \rangle$$

Final remarks

We have computed the contribution to the photon yield and v_2 from gluon fusion by a magnetic field during the early stages of a relativistic heavy-ion collision, where there is a large gluon occupation number below the saturation scale.

Agreement of the calculation with data is good in the lowest part of the spectrum: observed experimental fall between 0.5 and 1 GeV. Above 1 GeV the calculation overshoots the data spectrum and v_2 peaks for energy values $\sim \sqrt{eB}$

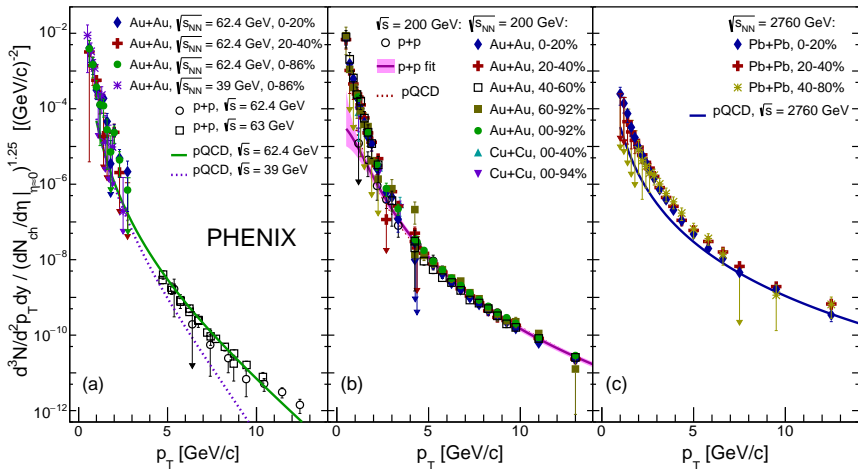
We have improved the approach for the 1L 2g1 γ vertex:

- constructed as $\Pi_{\parallel}^{\mu\nu} \times \tilde{\epsilon}_{\perp}^{\alpha\beta}$ which is required to have components in the transverse plane wrt \vec{B} ; when the $\omega_q^2 \gtrsim B$, this simple structure is spoiled
- we place two of the loop quarks in the LLL and the other one in the 1LL....new efforts to get a better/complete basis + yields and v_2

Work in progress: simulation and analysis to probe the magnetic field profile and evolution

¡GRACIAS!

PHENIX@BNL γ -yield, PRC 107 (2023)



Back

Effective temperature from direct-photon spectra

In the low p_T region, the inverse logarithmic slope of the photon yield, provides access to T_{eff}

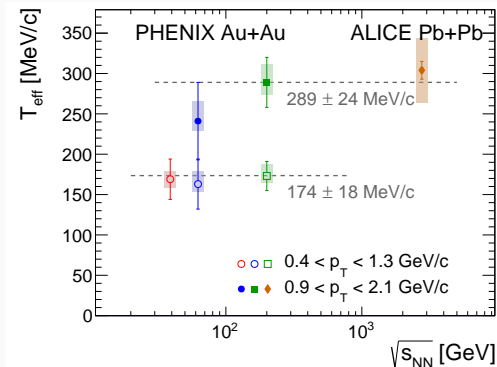
$$\frac{1}{2\pi} \frac{d^2 N}{dp_T dy} \sim \exp\left(-\frac{p_T}{T_{eff}}\right)$$

$$T_{eff} \sim 170 - 300 \text{ MeV}$$

greater than

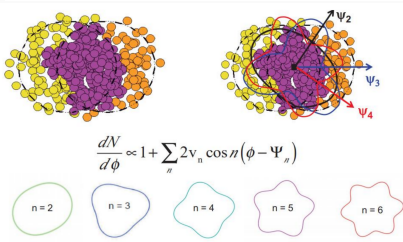
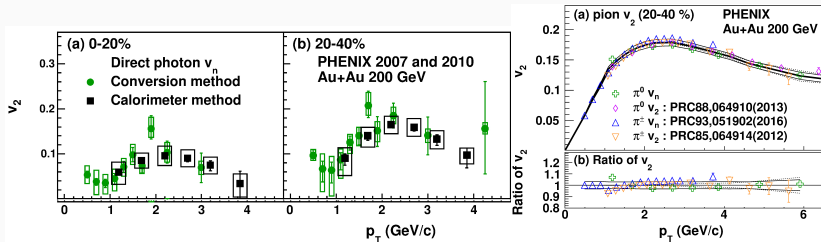
$$T_c \sim 155 - 170 \text{ MeV}$$

PHENIX@BNL, arXiv:2203.12354 [nucl-ex] (2022)



Back

Azimuthal asymmetries as large as those of hadrons



For “high” p_T : $v_2 \sim 0$ consistent with hard scattering source
 For “low” p_T : $v_2 \sim 0.15 - 0.2$ similar to hadrons

PHENIX@BNL, PRC 94 (2016), 1509.07758 [nucl-ex]

Back

Gluon fusion/splitting + strong magnetic field

The gluons and the photon are required to have parallel momenta

$$p^\mu = \omega_p(1, \hat{p}) = (\omega_p/\omega_q) q^\mu, \quad k^\mu = \omega_k(1, \hat{k}) = (\omega_k/\omega_q) q^\mu$$

+ gluon dist from glasma: simple model accounts for high occupation gluon number

$$n(\omega) = \frac{\eta}{e^{\omega/\Lambda_s} - 1} \quad \Lambda_s = 2\text{GeV}, \quad \eta = 3$$

+ the matrix elements for fusion/splitting

$$\begin{aligned} \overline{\sum_{c,p,f} |\mathcal{M}_{gg \rightarrow \gamma}|^2} &= \overline{\sum_{c,p,f} |\mathcal{M}_{g \rightarrow g\gamma}|^2} \\ &= \frac{2\alpha_{\text{em}}\alpha_s^2 q_\perp^2}{\pi\omega_q^2} \sum_f q_f^2 (2\omega_p^2 + \omega_k^2 + \omega_p\omega_k) \\ &\quad \exp \left\{ -\frac{q_\perp^2}{|eq_f B| \omega_q^2} (\omega_p^2 + \omega_k^2 + \omega_p\omega_k) \right\} \end{aligned}$$